Electronic Structure of Novel Superconductor $(Ca_{1-x}Sr_x)Pd_3P$

I Hase[1,*], T Yanagisawa[1], A Iyo[1], H Fujihisa[1], Y Gotoh[1], H Eisaki[1] and K Kawashima[2]

[1] National Institute of Advanced Industrial Science and Technology (AIST), Tsukuba, 305-8568, Japan
[2] IMRA Material R&D Co. Ltd., Kariya, Aichi 448-0032, Japan

*E-mail: i.hase@aist.go.jp

Abstract. In this paper we report the results of the first-principles calculations for $(Ca_{1-x}Sr_x)Pd_3P$ for various crystal structures observed in experiment. The calculated electron specific heat coefficient shows a good agreement with the experimental values. We found the centrosymmetric phase has a higher density of state at the Fermi level than that of the non-centrosymmetric phase. Possible parity mixing in the non-centrosymmetric phase is estimated as small in this system.

1. Introduction

Perovskite compounds with chemical composition ABX_3 (A, B: cation; X: anion) are used as a great number of useful materials due to their stability and the variation of elements. So-called anti-perovskite compounds AB_3X (A, B: cation; X: anion) have the same structure with ordinary perovskite compounds but the position of cations and anions are interchanged with each other. Anti-perovskite compounds also have rich variation of physical properties such as negative thermal expansion [1], topological crystalline insulator [2], and superconductivity with extremely high upper critical magnetic field H_{c2} [3].

Among them, recently found superconductor $(Ca_{1-x}Sr_x)Pd_3P$ has an interesting structural phase transition [4]. It has an anti-perovskite structure in all regions of Sr concentration x, but has inversion symmetry (centrosymmetric, CS) in the region where x is small and no inversion symmetry (non-centrosymmetric, NCS) in the region where x is large. Its T_c is large in the former (~3.5 K at x = 0.4) and small in the latter (~0.32 K at x = 0.75). The lack of inversion symmetry in antiperovskite superconductor reminds us the pioneer work for $CePt_3Si$ by Bauer *et al* [3]. In $CePt_3Si$, and also in another anti-perovskite-related superconductor Li_2Pt_3B [4], the possibility of enhancement of H_{c2} and lowering of T_c are suggested. On the other hand, the lack of inversion symmetry may not so important in other anti-perovskite-related superconductors Li_2Pd_3B and $Mg_{1.9}Rh_3P$ [4-7].

We are interested in the mechanism by which low T_c in the NCS phase occurs. There are two main possibilities: (i) In the NCS phase, the density of states at the Fermi level ($D(E_F)$) becomes smaller, and as a result, T_c becomes smaller. (ii) Parity mixing occurs in the NCS phase and T_c decreases.

To investigate these things, in this paper we performed a systematic first-principles band structure calculation of $(Ca_{1-x}Sr_x)Pd_3P$ using the experimentally observed crystal structures. We found that $D(E_F)$

in the CS phase is considerably higher than the NCS phase. Furthermore, we investigated the band splitting caused by spin-orbit interaction in the NCS phase, and found that this band splitting is considerably smaller than that of Li_2Pt_3B, which is known to have a large parity mixing. These results strongly suggest that the large change of T_c is mainly caused by the large change of $D(E_F)$.

This paper is organized as follows: The computational details are described in Section 2. The calculated results and the discussions are shown in Section 3. Finally we give some conclusions in Section 4.

2. Computational Details

2.1. Crystal Structures

$(Ca_{1-x}Sr_x)Pd_3P$ shows a structural phase transition with changing x, the concentration of Sr. $(Ca_{0.6}Sr_{0.4})Pd_3P$ has the orthorhombic structure (space group Pnma, #62) while $(Ca_{0.25}Sr_{0.75})Pd_3$ has the tetragonal structure ($I4_1md$, #109). We show a schematic picture of the crystal structure in Figure 1. Note that the former has an inversion center (centrosymmetric, CS), while the latter does not have any inversion center (non-centrosymmetric, NCS). Hereafter we call the former as CS-phase, and the latter as NCS-phase. The lattice constant and the atomic positions are reported in the previous work [7].

Sr-free $CaPd_3P$ has a related but another crystal structure (space group Aba2, #41) [8]. $CaPd_3P$ does not show superconductivity above 0.02K. This structure also does not have inversion symmetry.

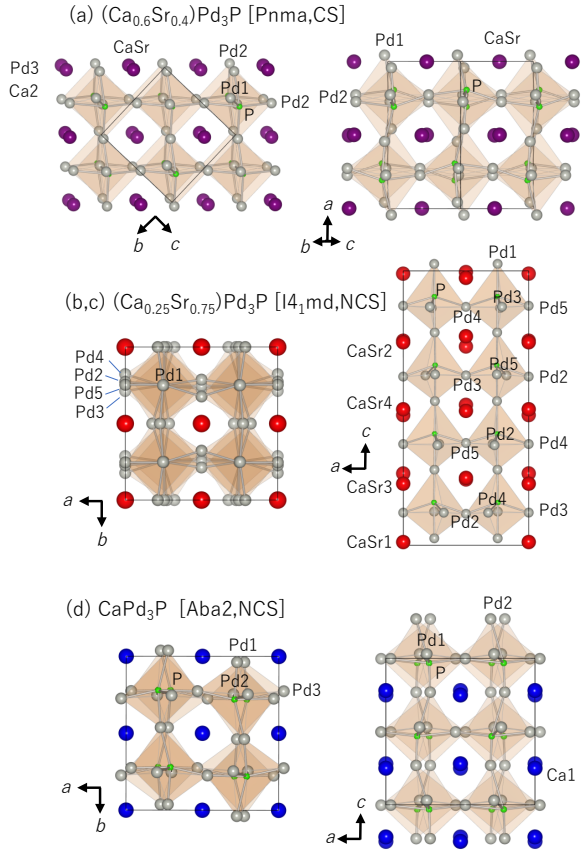

Figure 1. Schematic picture of the crystal structure of $(Ca_{0.6}Sr_{0.4})Pd_3P$, $(Ca_{0.25}Sr_{0.75})Pd_3P$ and $CaPd_3P$. The labels (a)-(d) correspond to the structure models in the following subsection.

2.2. Band Calculations

Since $(Ca_{1-x}Sr_x)Pd_3P$ is a mixed crystal, it is hard to calculate the electronic structure as it is. Therefore, we performed band calculations for the following four perfect crystal models:

(a) $CaPd_3P$_CS : $CaPd_3P$ using the crystal structure of $(Ca_{0.6}Sr_{0.4})Pd_3P$
(b) $CaPd_3P$_NCS : $CaPd_3P$ using the crystal structure of $(Ca_{0.25}Sr_{0.75})Pd_3P$
(c) $SrPd_3P$_NCS : $SrPd_3P$ using the crystal structure of $(Ca_{0.25}Sr_{0.75})Pd_3P$
(d) $CaPd_3P$_Aba2: $CaPd_3P$ using the crystal structure of $CaPd_3P$ (non-superconducting phase)

$(Ca_{0.6}Sr_{0.4})Pd_3P$ and $(Ca_{0.25}Sr_{0.75})Pd_3P$ are not only different in composition, but also have different crystal structure. However, comparing the above models, we can separate the two effects of composition and crystal structure. Namely, comparison between the model (a) and model (b) can focus on the crystal structure. Similarly, comparison between the model (b) and model (c) can focus on the chemical composition. We also added model (d) for discussing the structural stability of this system.

This calculation is based on the density functional theory (DFT) and the full-potential linearized augmented plane wave method (FLAPW), and the exchange-correlation potential is approximated by general gradient approximation (GGA) [9]. The whole calculation is implemented by the computer code WIEN2k [10]. The unit cell includes four formula units in model (a) and (d), and eight formula units in model (b) and (c). We used the parameter RK_{max}=7.0, and the muffin-tin radii are set as r(Ca/Sr) = 2.5, r(Pd) = 2.31 and r(P) = 1.8 a.u.

For self-consistent loop calculations, a 1000 k-points mesh were used for model (a) and (d), and a 250 k-points mesh were used for model (b) and (c), respectively. After convergence of potential, we performed the DOS calculation using 2000 k-points mesh.

The whole calculation is scalar-relativistic and spin-orbit interaction (SOI) is not included. However, as for the model (b) $CaPd_3P$_NCS, in order to discuss the effect of anisotropic spin-orbit coupling (ASOC), we performed additional calculation including SOI as a second variational procedure.

3. Results and Discussions

3.1. Structural Stability

As shown above, we calculated three structural models (a), (b) and (d) for the same compound $CaPd_3P$. Figure 2 shows the schematics of the total energy of them. The structure for the lowest energy is the model (d), which agrees with the experiment [6]. Interestingly, the more Sr content, the higher total energy. This may be due to the larger ionic radius of Sr compared with that of Ca.

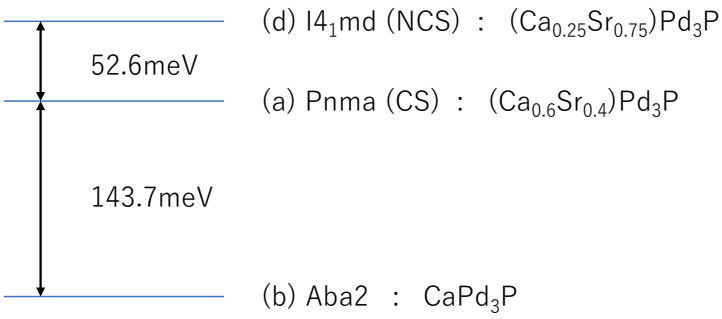

Figure 2. Total energy diagram for three structural models of $CaPd_3P$. Indices (a), (b), (d) correspond to those of the structural models described in subsection 2.2. We found that the model (d) has the lowest energy. These energies are per formula unit, i.e. $CaPd_3P$.

3.2. Density of States

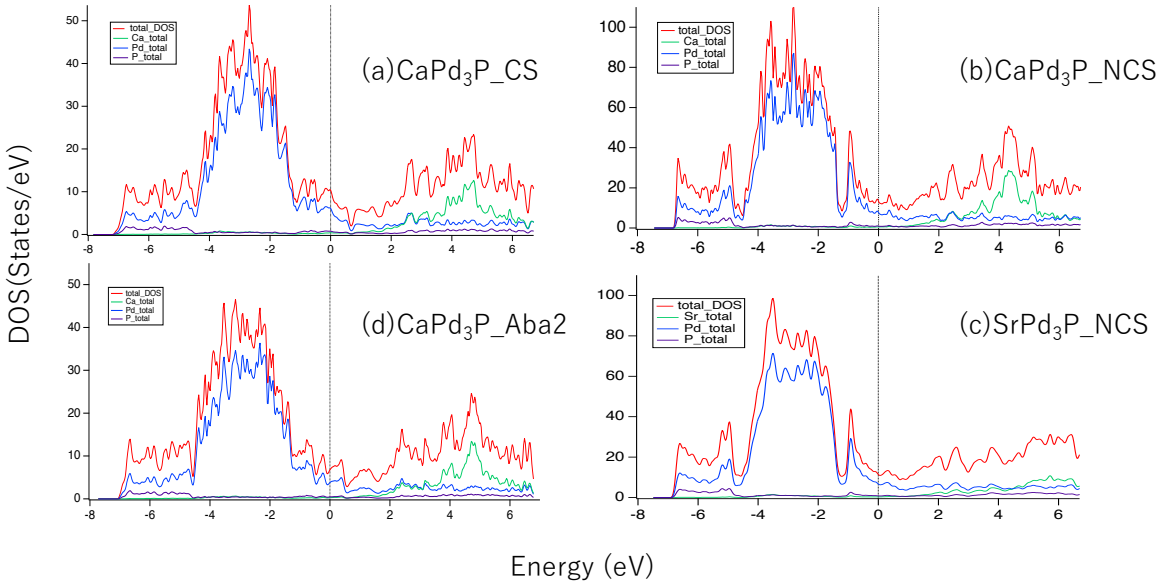

Figure 3. DOS curves of $CaPd_3P$ and $SrPd_3P$ for the structural models shown in subsection 2.2. The units of vertical axis are eV^{-1} per unit cell (i.e. 4 formula units in model (a) and (d), 8 formula units in model (b) and (c)).

We show the DOS curve of $CaPd_3P$ and $SrPd_3P$ with various structure models in Figure 3. The whole shape of the DOS curve does not change so much with structure models. The valence band mainly consists of the relatively narrow Pd-d band, and the Fermi level (E_F) is located at the top of the d-band. So the DOS at E_F (=$D(E_F)$) is moderate and magnetism is not expected like $MgCNi_3$ with the similar anti-perovskite structure [11]. This behavior is very similar to $SrPt_3P$ of which main component is Pt-d orbitals [12]. Note that model (b) and model (c) give almost identical DOS curve in the valence band region, even though the chemical composition is different. In this sense, as a first approximation, A-site

cations (Ca or Sr) only play a role for changing crystal structure due to the different ionic radii. Nevertheless, there is a difference in DOS near E_F depending on the model. E_F is on a peak in model (a) $CaPd_3P$_CS, while it is in a dip in models (b) $CaPd_3P$_NCS, (c) $SrPd_3P$_NCS and (d) $CaPd_3P$_Aba2. Correspondingly, $D(E_F)$ is 36.0 Ry^{-1}/f.u. in model (a), while $D(E_F)$ is 22.3, 17.7, 23.4 Ry^{-1}/f.u. in models (b), (c), (d), respectively.

Table I. Calculated results of $D(E_F)$ and γ_{calc} for various structure models. We also show the experimental results of γ_{expt} and T_c for $(Ca_{0.6}Sr_{0.4})Pd_3P$, $(Ca_{0.25}Sr_{0.75})Pd_3P$ and $CaPd_3P$. The last column shows the calculated attractive interaction parameter V using Equation (1).

models	$D(E_F)$ [Ry^{-1}]	γ_{calc} [mJ/molK^2]	γ_{expt} [mJ/molK^2]	T_c [K]	θ_D [K]	V [eV]
(a)$CaPd_3P$_CS	36.0	6.24	6.7	~3.5	182	0.0921
(b)$CaPd_3P$_NCS	22.3	3.88	3.0	~0.32	231	0.0908
(c)$SrPd_3P$_NCS	17.7	3.06				0.115
(d)$CaPd_3P$_Aba2	23.4	4.04		<0.02		

We show the calculated results of $D(E_F)$ and the electronic specific heat coefficient γ_{calc} in Table I, accompanied with the experimental results of the electronic specific heat coefficient γ_{expt}, and the superconducting temperature T_c for $(Ca_{0.6}Sr_{0.4})Pd_3P$, $(Ca_{0.25}Sr_{0.75})Pd_3P$ and $CaPd_3P$.
From Table I we can see that γ_{calc} of model (a) and γ_{expt} of $(Ca_{0.6}Sr_{0.4})Pd_3P$ are in good agreement. Similarly, γ_{calc} of model (c) and γ_{expt} of $(Ca_{0.25}Sr_{0.75})Pd_3P$ are also in good agreement. Therefore, we can conclude that the so-called mass enhancement due to electron-phonon or electron-electron interaction is small in this system.

From Table I we can also see a clear tendency that CS phase has a higher D, γ and T_c than the NCS phase (note that Aba2 is also a NCS space group). As described in Section 1, there are two possibilities that can explain the higher T_c in the CS phase: (i) larger $D(E_F)$ in CS phase causes higher T_c, as seen in BCS theory, and/or (ii) a parity mixing takes place and lowers T_c in the NCS phase.

Hereafter we look at the former possibility (i). The simplest form of the BCS equation is

$$T_c = 1.14\theta_D e^{-1/DV} \quad (1)$$

Where D is the DOS at E_F, θ_D is the Debye temperature, and V is an attractive interaction parameter. When we consider model (a) and set D = 36.0 Ry^{-1}, and use experimental values for $(Ca_{0.6}Sr_{0.4})Pd_3P$ as θ_D = 182 K and T_c = 3.45 K, we obtain V = 0.0921 eV for the CS phase. On the other hand, when we consider model (b) and set D = 22.3 Ry^{-1}, and use experimental values for $(Ca_{0.25}Sr_{0.75})Pd_3P$ as θ_D = 231 K and T_c = 0.32 K, we obtain V = 0.0908 eV for the NCS phase.

We found the ratio V^{NCS}/V^{CS} = 0.986, which is strikingly close to identity. This means that the simplest BCS theory works very well for elucidating the difference of T_c between the CS phase and the NCS phase. However, we should also note that if we use model (c) for representing D of the NCS phase, we obtain V_{NCS} = 0.115 eV. Therefore, this analysis has some ambiguity. Moreover, we should also note that the observed specific heat jump $\Delta C_{el}/\gamma T_c$ = 1.76 [13], which is considerably larger than the value ~1.43 predicted by the BCS theory. And we should consider that this system has multiple Fermi surfaces, as we will show later. These facts may affect the superconducting mechanism. Solving this problem is a future task.

3.3. Energy Band Dispersion and Anisotropic Spin-Orbit Coupling

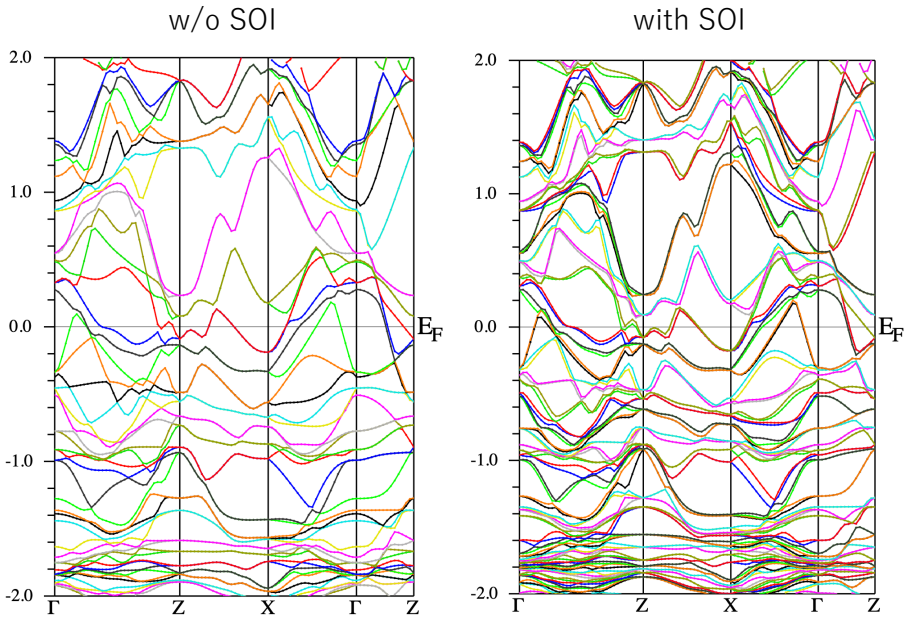

Figure 4. Energy dispersion curve of model (b) $CaPd_3P$_NCS near E_F. The left panel is the result when spin-orbit interaction (SOI) is not included, and the right panel is the result when SOI is included. The units of vertical axis are eV. Each band slightly (10 ~ 25 meV) splits by anisotropic spin-orbit coupling (ASOC) except for Γ point and the Brillouin zone boundary such as Z-X line. Note that there are two Z points in each panel, the left one denotes [1 0 0] and the right one denotes [0 0 1]. Namely, the left Γ - Z axis is parallel to k_x-axis, and the right Γ - Z axis is parallel to k_z-axis.

Next we discuss the energy band dispersion of $(Ca_{0.25}Sr_{0.75})Pd_3P$ in vicinity of E_F. Figure 4 is the band dispersion for the model (b) $CaPd_3P$_NCS. The left panel is the result without including spin-orbit interaction (SOI), and the right panel is the result with including SOI. Many bands cross E_F, which shows that this system has multiple Fermi surfaces. In the left panel, we can see that all the bands along Z-X line are doubly degenerated. This is due to the non-symmorphic feature of this structure, which is universally seen at the Brillouin zone boundary in non-symmorphic space group. Since the left panel does not include SOI, therefore these bands are actually 4-fold degenerated including spin degree of freedom.

When we include SOI, this 4-fold degeneracy along Z-X line is partly lifted and split into 2-fold + 2-fold bands. We found that this splitting is rather small as 10 ~ 25 meV, as seen in the right panel of Figure 3. The bands which are not on the Brillouin zone boundary also split by SOI, and the 2-fold (spin) degenerated bands split into 1-fold + 1-fold bands.

In the CS structure, this splitting is not appeared even SOI is switched on. In this sense, this splitting is often called as anisotropic spin-orbit coupling (ASOC), which is only seen in NCS structure. ASOC plays a crucial role to induce a parity mixing of the superconducting order parameter in NCS superconductor [14,15]. How much parity mixing occurs depends on the magnitude of ASOC. In Li_2Pt_3B, the band splitting due to ASOC is about 200 meV near E_F [16]. It is not easy to compare the accurate magnitude of ASOC between Li_2Pt_3B and $(Ca_{0.25}Sr_{0.75})Pd_3P$ directly, because the crystal structure is not

the same. However, it is clear that ASOC in $(Ca_{0.25}Sr_{0.75})Pd_3P$ is much smaller than that in Li_2Pt_3B. It is known that ASOC of Li_2Pd_3B is less than half of that in Li_2Pt_3B. ASOC is mainly determined by the atomic SOI of the principal orbital component of the band. Since Li_2Pd_3B and $(Ca_{0.25}Sr_{0.75})Pd_3P$ both include Pd-d orbital as the main component of the band near E_F, ASOC of these two compounds might show similar parity mixing. Therefore we can estimate that the parity mixing of $(Ca_{0.25}Sr_{0.75})Pd_3P$ is not so large as in Li_2Pt_3B, but is considered to be the same order as in Li_2Pd_3B.

As seen in the previous subsection, there is a clear tendency for T_c to increase as $D(E_F)$ or γ increases. Although the qualitative explanation using the simple BCS equation may be insufficient, we show the effect of the parity mixing in the NCS phase is not large as in Li_2Pt_3B. Therefore we conclude that the lower T_c in the NCS phase is not due to the parity mixing, but is due to the lower $D(E_F)$. More precise theoretical and experimental analysis is a future work.

4. Conclusion

We have calculated the band structure of novel superconductor $(Ca_{1-x}Sr_x)Pd_3P$ from first-principles using several crystal structure models. This system shows a structural phase transition when x is increased, and we have shown that the experimentally observed structure at $x = 0$ is energetically stable. It is shown that the calculated electron heat capacity coefficient is in good agreement with experiment. The difference of T_c between the two superconducting phases can be mostly explained by using the simplest BCS theory, though this analysis still remains uncertainty. The possible parity mixing due to the non-centrosymmetric crystal structure may be small in this system.

Acknowledgments

This work was partially supported by KAKENHI (Grant No. JP19K03731) from Japan Society for the Promotion of Science (JSPS).

References

[1] Takenaka K *et al*. 2005 *Appl. Phys. Lett.* **87** 261902
[2] Hsieh T H *et al*. 2014 *Phys. Rev.* B **90** 081112(R)
[3] Bauer E *et al*. 2004 *Phys. Rev. Lett*. **92** 027003
[4] Yuan H Q, Agterberg A F, Hayashi N, Badica P, Vandervelde D, Togano K, Sigrist M and Salamon M B 2006 *Phys. Rev. Lett.* **97** 017006
[5] Togano K *et al*. 2004 *Phys. Rev. Lett*. **93** 247004
[6] Iyo A *et al*. *Phys. Rev. Mater*. 2019 **3** 124802
[7] Hase I *et al*. 2019 *J. Phys. Conf. Ser.* **1293** 012028
[8] Iyo A *et al*. 2020 *Inorg. Chem*. **59** 12397
[9] Perdew J P, Burke K, Ernzerhof M 1996 *Phys. Rev. Lett.* **77** 3865
[10] Blaha P, Schwarz K, Madsen G K H, Kvasnicka D and Luitz J 2001 WIEN2k, *An Augmented Plane Wave + Local Orbitals Program for Calculating Crystal Properties* (Wienna: Vienna Univ. of Technology)
[11] He T *et al*. 2001 *Nature* **411** 54
[12] Subedi A, Ortenzi L and Boeri L 2013 *Phys. Rev.* B **87** 144504
[13] Iyo A *et al*. in preparation.
[14] Frigeri P A, Agterberg D F, Milat I and Sigrist M 2006 *Eur. Phys. J.* B **54** 435

[15] Samokhin K V and Mineev V P 2008 *Phys. Rev.* B **77** 104520
[16] Lee K -W and Pickett W, 2005 *Phys. Rev.* B **72** 174504